

# A novel design process of low cost 3D printed ambidextrous finger designed for an ambidextrous robotic hand

Emre Akyürek<sup>1</sup>, Tatiana Kalganova<sup>1</sup>, Mashood Mukhtar<sup>1\*</sup>, Luke Steele<sup>1</sup>, Michal Simko<sup>1</sup>, Alisdair Nimmo<sup>1</sup>, Luke Kavanagh<sup>1</sup>, Leonid Paramonov<sup>2</sup>, Anthony Huynh<sup>1</sup> and Stelarc<sup>3</sup>

Department of Electronic & Computer Engineering  
Brunel University, Uxbridge, UB8 3PH, London, United Kingdom<sup>1</sup>  
Norwegian University of Science and Technology, No-7491 Trondheim, Norway<sup>2</sup>  
Curtin University Perth, Kent St, Bentley WA 6102, Australia<sup>3</sup>

\*Corresponding author: Mashood.Mukhtar@brunel.ac.uk  
[www.dea.brunel.ac.uk/ambi-hand/](http://www.dea.brunel.ac.uk/ambi-hand/)

*Abstract:* - This paper presents the novel mechanical design of an ambidextrous finger specifically designed for an ambidextrous anthropomorphic robotic hand actuated by pneumatic artificial muscles. The ambidextrous nature of design allows fingers to perform both left and right hand movements. The aim of our design is to reduce the number of actuators, increase the range of movements with best possible range ideally greater than a common human finger. Four prototypes are discussed in this paper; first prototype is focused on the choice of material and to consider the possible ways to reduce friction. Second prototype is designed to investigate the tendons routing configurations. Aim of third and fourth prototype is to improve the overall performance and to maximize the grasping force. Finally, a unified design (Final design) is presented in great detail. Comparison of all prototypes is done from different angles to evaluate the best design. The kinematic features of intermediate mode have been analysed to optimize both the flexibility and the robustness of the system, as well as to minimize the number of pneumatic muscles. The final design of an ambidextrous finger has developed, tested and 3D printed.

*Key-Words:* - Ambidextrous finger, Finger design process, Low cost 3D printed finger, Ambidextrous finger concept, Robotic finger design

## 1 Introduction

It is a believed fact that human hand is the most perfect engineered product of nature. Nearly all scientific disciplines including medical and engineering are seemed to be inspired by nature itself. Human hand has a complicated structure and it performs actions as instructed by brain via nerves [1]. Human hand is one of the most complex organs of our body. Due to high level of complexity involve in designing such hands, previous attempts were focused on meeting specific set of applications i.e. prosthesis, humanoid and manipulator for industrial and astronautic purposes [2]. For instance, a five fingered robotic hand also known as Belgrade/USC Hand [3] is built to offer better grasping

tasks and capable of autonomous adaption. Similarly, a UTAH/MIT [4] hand jointly developed by University of Utah and the Artificial Intelligence laboratory at the MIT is intended to function as a general purpose research tool for the study of machine dexterity and teleoperation system. A five finger Robonaut hand is developed by NASA [5] to meet the requirement of extra vehicular activities.

Development of industrial robotics started in 1960s which resulted in production of several grippers. Due to number of limitations associated with these grippers, research focus was diverted in developing multifinger robotic hands [6], [7], [8]. Much work has been done to develop multifinger robotic hands namely the Stanford/JPL hand (1983) [9], the UTAH/MIT hand developed

in 1983 (1986) [4], the Belgrade /USC hand developed in 1988 (2000) [10], the Barret Hand (1988) [11], the Robonaut hand (1999) [5], the Gifu hand (2001) [12], the DLR hand II (2001) [13], the BUAA Hand (2001) [14], the MA-I hand (2004) [15], the UB hand III (2005) [16], the RCH-I hand (2006) [17], the Elu 2 Hand (2010) [18], the Shadow Robotic hand (2013) [19] and many more [20].

Robotic fingers have always been considered as one of the most active research area of robotics. Since fingers play vital role in determining the performance of a hand, it is always been a focus of Engineers. A trend to design underactuated finger has been noted throughout the literature [21]. The underactuated design offers greater degree of freedom than the number of actuators. Hence; this makes the overall design simple and easily controllable.

The concept of underactuation is first introduced in patent filed by Itoh, F [22]. The scope of the original concept was extended in great details by Hirose and Umetani [23] [24]. There are two types of underactuated fingers found in the literature; Fingers based on linkages and finger based on tendon actuated. It is noted that linkage based fingers are better suited and widely used in large grasping forcing applications while tendon transmission seems to be preferred in prosthesis [25]. The Belgrade/USC hand [3] was one of the very first designs which feature the underactuation technique between fingers. Four of the fingers are driven by two actuators through seesaw mechanism. Similarly Barret hand offers 8 degree of freedom with just 1 actuator and SDM hand offers 8 degree of freedom with 1 actuator.

Robotic Hands	Mechanical Features of Hands				
	No of actuator	No of Fingers	No of DOF	Range of motion	Speed of motion
Tokyo hand, University of Tokyo 1999 [26]	16	5	12	~ human hand (Dexterous hand)	~ human hand
Peter Scarfe, 2006 [27]	15	5	7	~ human hand (Dexterous hand)	~ human hand
J. Sancho-Bru et al [28]	25	5	20	~ human hand (Dexterous hand)	N/A
D. Wilkinson et al. [29]	31	5	20	~ human hand (Dexterous hand)	N/A
Y. Honda et al, 2010 [30]	25	5	17	~ human hand (Dexterous hand)	N/A
The ExoHand [31]	26	5	20	~ human hand (Dexterous hand)	~ human hand
The Shadow Hand [32]	40	5	20	~ human hand (Dexterous hand)	0.5 x human hand
Ambidextrous Robot hand (Proposed)	17	5	14	2 X human hand (Ambidextrous hand)	> human hand

Table 1: Mechanical Hands and their features are listed against our proposed hand.

With the passage of time, number of fingers and henceforth, degree of freedom has increased [33]. Initially, 3 finger hands are developed i.e. Stanford /JPL hand [9] and Barret hand [11], moving to 4 fingers as seen in DLR hand I, DLR hand II [13], DIST hand [34] and Utah/MIT hand [4]. The increase in number of fingers has continued until it reaches its human counterpart. Almost all the late 1990s hands have five

fingers i.e. Robonaut hand [5], Tuat/Karlsruhe hand [35], Ultralight hand [36], Gifu hand [12], Bebionic hand III [37], Shadow dexterous hand [19]. Mechanical features of various hands actuated by PAM are listed in table 1.

Generally, range of movement of fingers has also improved over the period. This improvement can be noted in recent development of Shadow hand (2013)

[19] which have been designed to have a range of movement equivalent to that of a typical human being. It offers 0-90 degree for the first, second and third joint and -20-20 degree for the fourth joint of a finger. Similarly, weight of the finger is also reduced to make the overall hand feel lighter. The finger of universal hand (2012) [38] only weighs about 0.250kg. This is a slightly less than DLR hand II (2001) [13] finger which weighs around 0.375kg.

Mainly two types of actuators are used in the past to control the fingers; Motors and PAMs. It was noted that system which employs built-in motors lacks flexibility feature on the other hand those using PAMs makes system complex and less attractive to end users. Some key points have been observed about the behaviour of fingers. It is deduced that fingers designed with all independent joints are easy to control and offer greater degree of freedom than fingers with coupled joints. However, coupled joints help fingers to grasp object of various sizes and shapes. Hence, coupling augments the dexterity of hand.

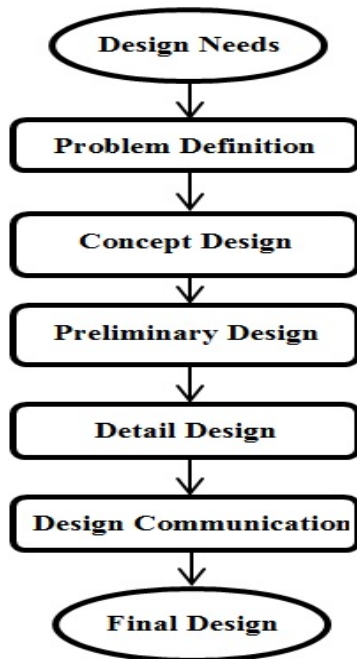


Figure 1: Design process of a product. [8].

Although number of dexterous fingers has been designed in the past but ambidextrous nature of finger has not investigated in robotics previously. In this paper, we are presenting a novel design of an ambidextrous finger driven by pneumatic muscles. Requirements for the finger design include efficient grasping feature, use of minimum number of muscles, larger range of movement, stable control, and cheapest manufacturing reliable material. The ambidextrous design allows a significant reduction in the implementation of resources yet maintaining the flexibility, stability and reliability of the system. The finger is capable of performing both left and right hand finger movements. Later the final design

of finger has been integrated into ambidextrous robot hand [39].

Jorge et al presented a design process of a product in [8]. Similar process is employed to design our ambidextrous finger. The full design process is shown in Fig.1.

## 2 Design of Ambidextrous Finger

In order to accurately design an anthropomorphic ambidextrous nature robotic finger, four stages design process is employed. Each stage focuses on specific tasks. Design A mainly aims to validate the choice of the material and to consider the reduction of the friction. Design B allows testing of different tendon configurations and multiple sizes of pulleys. Experiments are performed to confirm that it is possible to drive an ambidextrous finger with three PAMs. With the use of offset pulleys, maximum muscle range is tested. Design D reveals accurate geometrical features with the aim of rectifying the imperfections of previous designs. The more efficient solutions were combined to design a final version of an ambidextrous finger. Aim of each design is presented in table 2.

Design (s)	Aim of designs
Design (A)	Validate the choice of the material and reduce the friction.
Design (B)	Test different tendon configurations and multiple sizes of pulleys. Experiments were done to confirm the possibility of driving an ambidextrous finger with three PAMs.
Design (C)	Impact of offset pulleys on the muscle's range.
Design (D)	Finding accurate geometrical features with the aim of rectifying the imperfections in the previous designs.
Unified Design (Final)	Selection of best combination and incorporation of position sensors in the phalanx.

Table 2: Aim of each design is discussed briefly.

### 2.1 Design A: Choice of material

The design A is made of steel plates, with tendons routed through smooth cylindrical surfaces with or without grooves to direct the tendon along the surface and was exclusively modeled for a four-tendon routing scheme. Design of the robotic finger took cues from robotic hands that had more open structures, without fixed path routing, such as the DLR hands [13] and the early UB Hands [16]. This allows easy manufacturing and assembly as well as reducing tendon friction by minimizing contact points. An emphasis was also put on

creating a strong external skeletal structure capable of withstanding large forces from the muscles whilst allowing plenty of space for the internals; pulleys, tendons and sensors etc.

As shown in Fig.2, the skeleton structure of the finger is made of a solid steel plate. Another key feature of the design includes the coupling of distal and medial phalanxes using tendons with a 1:1 ratio of movement and winding around pulleys to avoid lift off. Low friction pulley turn with and without grooves for tendon guidance, which permits to evaluate how important is the tendon channeling. The pulleys are fixed using circlips or shouldered pins for joint pulleys. A circlip and rod design is trialed for mid-phalanx pulley insertion where the pulley is required to remain stationary. The tendon routing is shown in Fig.3. A linear and intuitive control is allowed by a symmetrical four tendon design with minimal lift and even force distribution on either side of the finger.

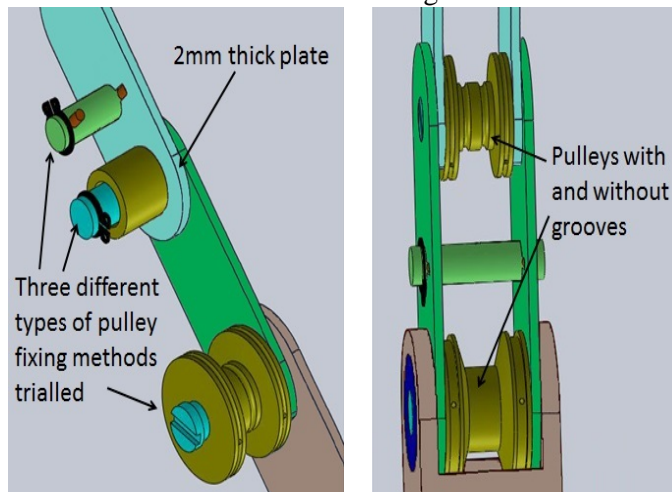


Figure 2: Design A, CAD assembly of pulleys.

Several key issues have been exposed with this design and different solutions were found and used to inform later designs. Testing tendon wrapping shows that even the smallest amount of friction created by the wrapping causes a moment arm about the preceding joint. Securing tendons centrally using thread interference is found to be unsatisfactory. Circlips are found to be a space effective way of securing pins laterally. The use of bearings is found to be extremely effective in reducing friction whilst also reducing the likelihood of manufacturing error in such a critical area of the design. The metal skeleton structure is a valid design idea but testing proves that rapid prototyping ABS plastic is strong enough for this application. Although the tendons are resistant they have poor wear resistance and sharp threaded edges damage them causing the tendons to break under high tension. Besides, because of the compliance of PAMs it has been decided the central routing of tendons is not an important factor.

Among the different material tested for tendons, the one with the lowest coefficient of friction was Dyneema 0.51, which shows a 58% reduction of friction compared to the less efficient tested material (Carbo Flex). Tendon material is discussed in section 3.1. The different kind of pulleys are found to be a satisfactory design solution provided there is suitable tendon guidance either side of said pulley. These key issues are taken into account for the following models. Their design will also include brass pulleys which, combined with Dyneema tendons, reduce the friction by 86.7% compared to rapid prototyping parts.

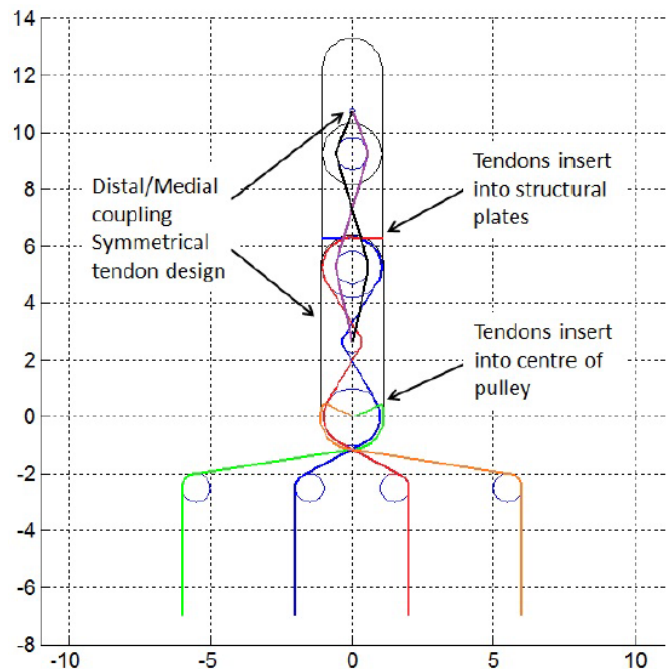


Figure 3: Design A, Matlab model showing tendon routing.

## 2.2 Design B: Tendon routing investigation

The design B is made of an aluminium skeleton, phalanges made up from two aluminium sheets, brass pulleys and rapid prototyping parts printed from ABS plastic. The main key concern of this prototype is its adaptability. The model aims to combine robustness with flexibility and to feature several options for tendon routing and interchangeable pulleys. This approach would provide a strong platform for investigation and experimentation for the unified design. It is assumed that the fused deposition modelling parts, through their layered deposition process, would result in coarse parts with high coefficients of friction.

The concept can be seen in Fig.4 and Fig.5. The central structure makes use of two sheets of aluminium held together by a series of pins and fasteners. Thus the core of each phalanx is mainly hollow. An internal cavity is designed into the finger to allow investigation of multiple routing options without incurring reworking of CAD models and sending new parts to the 3D printer. Additionally, the cavity is designed to house wiring and



any sensor circuitry. Stainless steel fasteners are secured into the tapped pulley bushes that hold the assembly together. The plastic rapid prototyping parts are printed from ABS material. The different materials are selected for their low friction properties with the aim to minimize losses in the joints. Nylon washers are used between the aluminium plates to avoid sliding contact between any two fused deposition modelling parts. Pulleys' positions are secured using pins with circlips. Internal bushes are machined to size from silver steel, which together with the brass pulleys provide good friction performance.

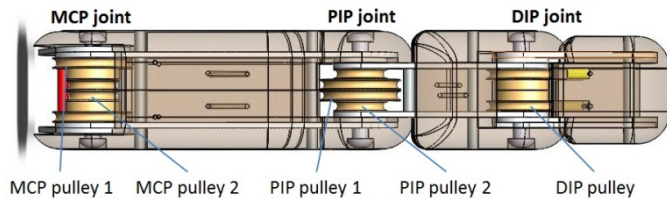


Figure 4: Design B, top view of final concept.

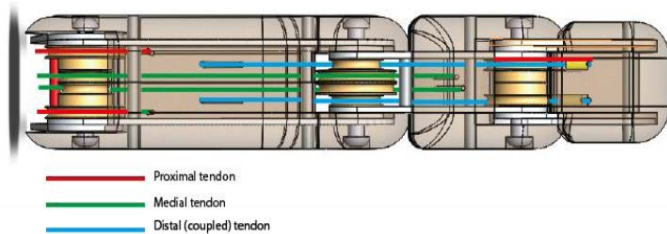


Figure 5: Design B, internal routing of tendons (Top View).

Among the different possible configurations of this design, it is noted that the required specifications can be reached both with a four and three tendons configuration. The final tendon configuration is illustrated in Fig.6. The proximal tendon is inserted towards the outer face of the finger. This reduces any uneven force distribution on the metacarpophalangeal joint. The middle phalanx is routed around a reduced diameter pulley in the same joint, to minimize any tendon extension resulting from the coupling of the middle and proximal phalanges. Tendons are retained in the pulley channel/groove by two pulley pins. The pulley diameter is maximized to increase the available torque for the middle phalanx. The routing is achieved through insertion of tendons into the proximal phalanx, routed through the middle phalanx and ending at an adjustable insertion point in the distal phalanx (Fig.7).

To replicate the range of motion of the distal phalanx compared with the medial phalanx, a pulley ratio is used between the PIP and DIP joints to achieve the desired ratio of angles between the two fingers. As the middle phalanx has a greater range of angular motion than the distal ( $100^\circ$  instead of  $65^\circ$ ), the pulleys are required to step down the relative coupled motion of the distal phalanx, to wit a pulley ratio of about 1.5. Even though

the full range of movements is achieved, testing of the finger reveals some weak points of the structure. The sheet aluminium does not reach the required accuracy. This is partly due to 'tolerance creep' in the manufacturing process and partly due to the softness of the material, resulting in some deformation during assembly of the prototype. These inaccuracies result in a higher than expected frictional performance, more as a result of misalignment of components than poor choice of materials.

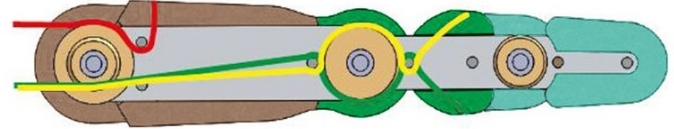


Figure 6: Design B, three tendons routing configuration.

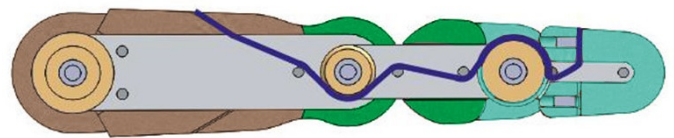


Figure 7: Design B, passive tendon routing to distal phalanx.

It is also noted that the rapid prototyping parts are strong enough to endure the PAMs' contraction. Consequently the metal skeleton can be removed to increase the thickness of the rapid prototyping parts instead of. These weak points are taken into account and corrected for the next designs.

### 2.3 Design C: Maximization of the range

The design C is made of ABS plastic and is composed of seven pulleys made of brass (Fig.8 and Fig.9). The pulley of the medial phalanx is slightly shifted by 2 mm towards the centre of the phalanx, which creates a variable radius of the pulley. The diameter of the pulleys is defined according to the muscle extension parameters and overall prediction of the finger behaviour. The tendon routing is illustrated on Figure.8 and is designed for a three muscles configuration. In this method two tendons are responsible for the movement of both medial and proximal phalanges. Thus a higher force is required for the single PAM to overcome the opposite force of the two stretched PAMs. This high muscle extension is caused by routing the tendon over the knuckle pulleys and is determined by the size of pulleys.

This initial model achieves a full range of motion; however it does not generate enough force to grasp objects because of the stretching force provided by the antagonist muscle. Hence the concept is designed with the aim to increase the performance and to maximize the grasping force. This configuration generates a higher torque for the active muscle and at the same time reduces the torque for the opposing muscle. The new pulley arrangement achieves the force ratio of 1:1.78,

thus to overcome the muscle opposing force of 10N it is required to generate only 5.8N.

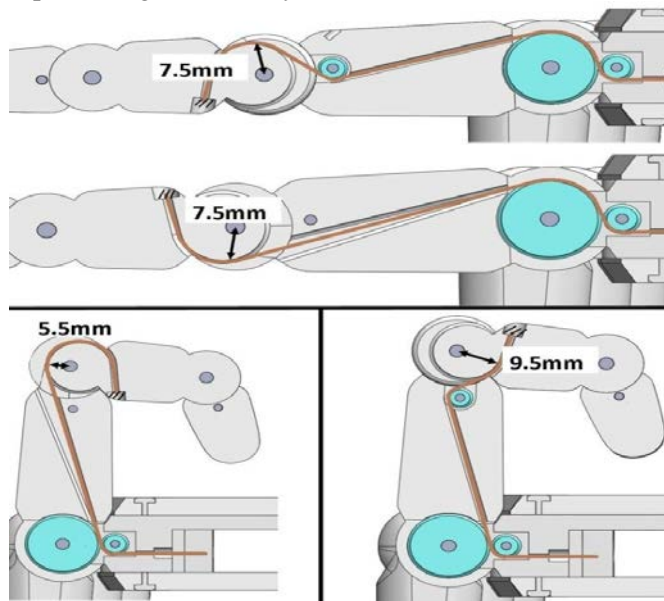


Figure 8: Design C, final design with the offset pulleys configuration.

In order to achieve the correct functionality of this coupled movement, it is necessary to design a mechanism that allows stretching the tendon inside the phalanges. The most appropriate technique is achieved by fixing the tendons with a grub screw into the Distal Phalanx. The other tendons are fixed via nodes, which do not require extra cost or manufacturing. The finger joints are assembled using shaft press fit.

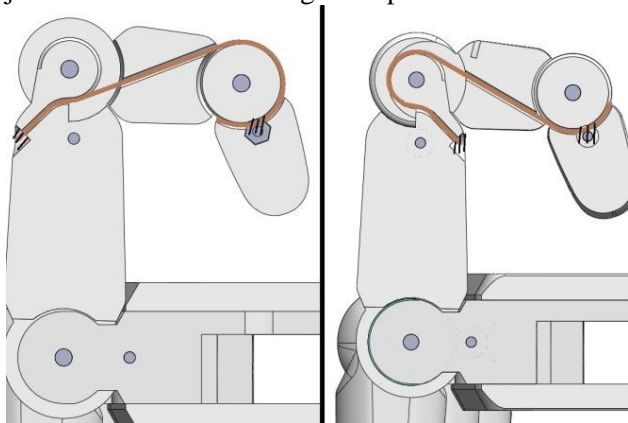


Figure 9: Design C, coupling of medial-distal phalanges

After testing, the design revealed that further improvements were required. The pulley controlling the proximal phalanx should be directly implemented inside the phalanx to increase the performance of the movement. Some of the pulleys can also be built in ABS to allow the structure of a phalanx not to rotate. Besides, it is fast to machine and more durable. It is suggested to generate the same size pulley with the variable radius which would increase the torque of the muscle in active mode and reduce the force of the muscle extension in the reverse motion. It is also

observed that some friction is present in the knuckles and hence it is believed that the performance of the finger can be increased by implementation of the ball bearings into the finger joints. These issues will be solved in Design D.

## 2.4 Design D: improvement of the performance

The design D is made of fused deposition modeling printed in ABS and is exclusively based on a three-tendon routing scheme (illustrated in Fig.10). This configuration offers complete constraint of a two-degree of freedom system with three tendons: one tendon (#1 as in Fig.10) constrains proximal phalanx rotation only, while the other two tendons (#2 and #3 as in Figure.10) are routed such that changes in their relative length cause middle phalanx rotation, and uniform motion opposes the rotation caused by tendon #1 as in Fig.10. The distal and proximal phalanges are connected via two tendons (red and black) so as to couple the movement of the distal phalanx relative to the proximal (Fig.11).

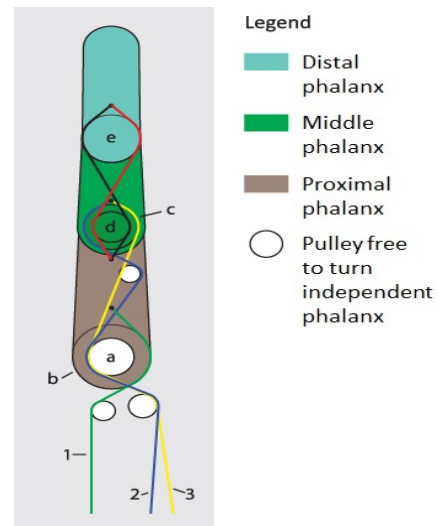


Figure 10: Design D, tendon routing scheme.

In order to maximize the performance of the finger, pulley diameters are chosen to utilize as much of the active range of the muscles as possible (first determined as 53mm). Additionally, because of the inherent asymmetry of the three-tendon scheme, the proximal phalanx diameter around which tendon #1 is wrapped (*b*) is adjusted to be as close to twice the diameter of pulley *a* as possible – the extent to which this was possible was dictated by the packaging constraints for the peripheral pulleys below the proximal.

The target angle ranges for the proximal/knuckle and proximal/middle joints were both 200°. Denoting the radii of pulleys *a*, *b* and *c* as  $r_a$ ,  $r_b$  and  $r_c$  respectively, the required extension distance of tendons #2 and #3  $l_{2,3}$  and the required extension distance of tendon #1 as  $l_1$ , it can be seen that:

$$l_1 = r_b \frac{200}{180} \pi \quad (1)$$

To minimize the number of large muscles in the finger and given that a smaller muscle extension is 38 mm  $r_b$  is calculated as:

$$r_b = 38 \times \frac{180}{200\pi} \sim 10.5 \text{ mm} \quad (2)$$

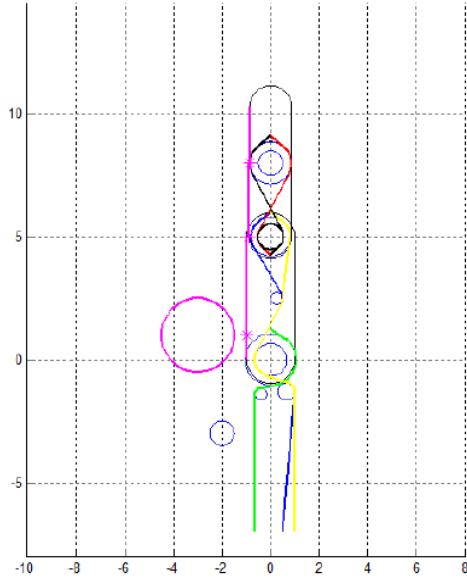


Figure 11: Design D, tendon routing scheme, pulley diameters, positions and phalanx lengths to scale.

To maximize the torque on the middle phalanx, the diameter of pulley  $c$  must be maximized. Because the extension requirement for tendons #2 and #3 is much bigger than that for tendon #1, larger muscle sizes are used for those tendons, conservatively assuming a maximum extension distance  $l_{1,2}$  of 50mm. It can also be seen that:

$$l_{1,2} = \frac{200\pi}{180} r_a + \frac{200\pi}{180} r_c \quad (3)$$

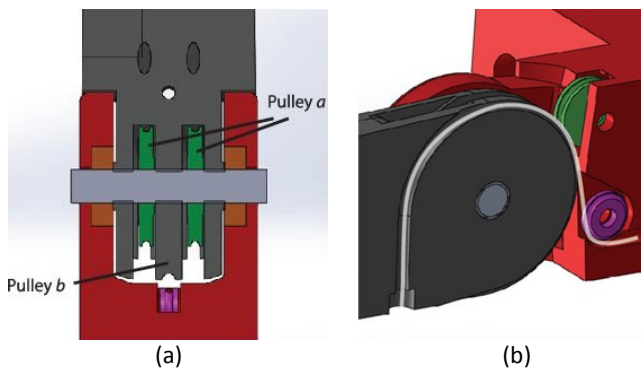


Figure 12: Design D, where (a) is the proximal/knuckle joint and (b) is tendon #1 routing.

As a radius of 8mm is appropriate for  $r_c$ ,  $r_a$  can be calculated as:

$$1. \quad r_a = l_{1,2} \times \frac{180}{200\pi} - r_c = 6.32 \text{ mm} \quad (4)$$

A cross section of the proximal/knuckle joint and the tendon routing is shown in Fig.12. The axle of 4mm in diameter is constrained in the proximal phalanx by friction fit, and 4x7x2.5mm bearings hold the axle in the knuckle. The pulley  $b$  is placed at its center, and the two  $a$  pulleys sit on either side of  $b$  in the spaces between the prongs. The pulleys are machined from brass, and feature a small boss around the center to minimize the surface area of in contact with the fused deposition modeling surface. Gathering the observations done on each design and comparing the advantages to the inconveniences, the next session discusses the kinematic analysis.

## 2.5 Unified Design: Final Design

Three tendons routing scheme was proved most appropriate after testing the kinematic ranges of fingers (fig.13 (f)). Therefore, three tendon scheme was used in the final design [40]. Off set pulleys were implemented in the medial phalanx base utilizing bearing based joints to achieve maximum compression torque while minimizing the spring force of the muscle.

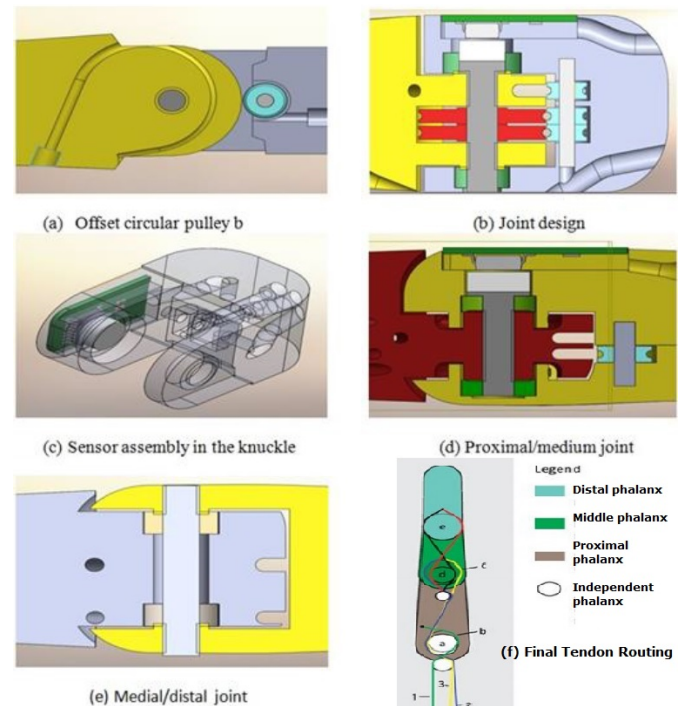


Figure 13: Different joints offset pulley and sensor assembly is shown.

The design of the proximal/knuckle joint is shown in Fig.13 (d). The axle (dark grey) is 4mm in diameter with an enlarged 6mm diameter boss at one end which butts up against the magnet (white) – the boss and magnet are both held concentric within a 6x10x2.5mm bearing (green). The lower side of the boss - facing the 4mm part of the shaft - butts up against the proximal phalanx body. The



6x10x2.5mm bearing is held in a recess in the knuckle. The other end of the axle is held in a 4x7x2.5mm bearing, which in turn sits in a suitably sized recess in the knuckle. The proximal phalanx (yellow) features bosses to ensure the phalanx is in contact only with inner races of the bearings – the outer races sit in contact with the knuckle. Note that these features are intentionally modeled oversize to allow for manual filing to the required fit – necessitated by the tolerances achievable by the 3D printer. Pulley *b* is integrated into the surface of the proximal phalanx. The two red pulleys are the *a* pulleys, and are machined from brass with a loose sliding fit to ensure free rotation on the axle.

The proximal / medial joint (Fig.13 (d)) is formed around a 3mm axle (dark grey) machined from mild steel, constrained by two bearings (green). The axle is held by friction fit to ensure rotation with the medial phalanx. The top of the axle features an enlarged (6mm diameter) boss that sits against the inner race of the upper bearing. The magnet (white) is attached to the axle boss with adhesive– either slow drying cyanoacrylate or fast drying epoxy, to provide sufficient curing time to be able to ensure concentricity – a

difficulty with regular cyanoacrylate. The proximal phalanx contains a recess to provide sufficient clearance for the magnet. The sensor assembly is again retained in place by friction fit, and can be glued in place after assembly. The tendon #2 reversal pulley (cyan) sits on a 2mm silver steel axle located inside the proximal phalanx. The distal/medial joint (Fig.13 (e)) utilizes a 3mm shaft constructed from silver steel, mounted in two 3x6x2.5mm bearings. These bearings are held within the distal phalanx (grey), due to its greater thickness. The lower groove in which the coupling tendon run in the distal phalanx is displaced significantly to one side as a consequence of the asymmetry of the proximal / medial joint, causing the two tabs of the medial phalanx (yellow) which form the joint to be comparatively thin (approximately 3mm).

### 3 Kinematic Analysis

The main challenge of designing ambidextrous fingers is to reach the full range due to PAM’s extension. Consequently, the main aims are to evaluate the kinematic performance of the fingers’ prototypes and check the achievements of their theoretical ranges.

Key Features of all Designs				
Design A	Design B	Design C	Design D	Unified Design
1. Four tendon routing 2. All metal construction 3. Test-bed for unique tending fixing methods 4. Bearings in knuckle, bearing-less design in other joints. 5. Trialled wrapped pulleys 6. Open tendon routing.  7. Distal and medial phalanxes were coupled using tendons with a 1:1 ratio of movement and wrapping around pulleys to avoid lift off.  8. Low friction brass pulleys were turned with and without grooves for tendon guidance to see how important tendon channelling is.	1. Metal skeleton with ABS superstructure.  2. Open internal structure to facilitate easy (and reconfigurable) tendon routing.  3. Can accommodate 3 or 4 tendon configuration.  4. Reconfigurable pulley diameters. 5. Silver steel bushings for axles.	1.3-Tendon routing  2. Bearing less design with joint clearances carefully adjusted for low friction operation.  3. Uniform pulley diameters at base of proximal, all metal (brass).  4. Simplified proximal/distal coupling adjustment.	1. All ABS design with silver steel axles  2. Bearings used in all joints  3. Three tendon design  4. Distal/proximal coupling adjustment through individually adjustable screw constraint.  5. Pulley diameters optimised to maximise torque at joints.  6. Pulley surfaces integrated into ABS where possible.	1. Best Design Selected and position sensing in the phalanx joints.  2. Position Sensors Incorporated.  3. Three Tendon Routing Scheme  4. Offset Puleys  5. Bearing base joints to achieve compression torque.

Table 3: Key features of all designs are listed.

Design A implements bearings in the proximal base, and exhibits strong behaviour in that region. However the proximal/medial joint displays significant friction and an unanticipated effect is to create a moment on the

proximal due to the use of intermediate tendons in the proximal base, in much the same way as the three-tendon design creates a moment on the proximal phalanx by constraining the motion of the two tendons which wrap around the proximal base pulleys. The main



observation here is that intermediate pulleys are undesirable in four-tendon designs and their diameter should be minimized – their effect is to facilitate an induced torque if any friction is present in the proximal/medial joint. Besides, the finger’s mass appeared too great for the muscles to successfully actuate.

Design B operates through its complete design kinematic range but it exhibits significant friction in

areas of its motion due to minor design/manufacture issues. The range of designs A and B is evaluated in Table II. Even though the flexibility of the design appears attractive, it is decided to pursue a three-tendon design. Despite the difficulties it adds to control, its innovative nature and the potential reduction in number of muscles makes it attractive. Tendon configurations of all designs are listed in table 4.

	Tendon Configuration
Design A	Tendons routed through smooth cylindrical surfaces with or without grooves to direct the tendon along the surface and was exclusively modelled for a four tendon routing scheme.
Design B	The routing is achieved through insertion of tendons into the proximal phalanx, routed through the middle phalanx and ending at an adjustable insertion point in the distal phalanx.
Design C	In design C, two tendons are responsible for the movement of both medial and proximal phalanges. Thus a higher force is required for the single PAM to overcome the opposite force of the two stretched PAMs. This high muscle extension is caused by routing the tendon over the knuckle pulleys and is determined by the size of pulleys.
Design D	This configuration offers complete constraint of a two-degree of freedom system with three tendons: one tendon constrains proximal phalanx rotation only, while the other two tendons are routed such that changes in their relative length cause middle phalanx rotation, and uniform motion opposes the rotation caused by tendon 1. The distal and proximal phalanges are connected via two tendons so as to couple the movement of the distal phalanx relative to the proximal.
Unified Design (Final Design)	After initial testing to establish the kinematic ranges of the fingers, it was decided to proceed with an implementation of the three tendons routing scheme, implementing the offset pulleys in the medial phalanx base, but utilising bearing-based joints. In addition to that a similar spiral or offset pulley was implemented for the base of the proximal phalanx, with the intention of maximising compression torque but minimising the spring force of the muscle at the opposite extreme of motion.

Table 4: Comparison of tendon configuration of all designs is listed.

Contrary to four tendons designs, full kinematic range could not be achieved for the three tendon configuration during first tests. In the intermediate position illustrated in Fig.14, all three-tendon fingers could achieve their full range of motion. However, when the proximal phalanx is at its most anti-clock wise (such as (e) and (f) in Fig.15), the proximal is driven to this position by tendons #2 (as in Fig.14) and #3 (as in Figure.14) acting in unison. While in this position tendon #1 is at its most extended and functions like a spring, exerting a clockwise torque. When the medial phalanx is moved in this region, either tendon #2 (as in Fig.14) or #3 (as in Fig.14) is relaxed while the force in the other is increased (within the limit of the muscle). The net anti-clockwise torque due to the two tendons on the proximal phalanx decreases, and the proximal phalanx lifts upwards.

The same phenomenon can be seen at the other extreme of motion. When the proximal is in the fully clockwise position it is held there only by the tension in tendon #1, and muscles #2 and #3 are extended such that

when the tension in one is increased to move the medial, the net torque is sufficient to rotate the phalanx several

degrees clockwise. The magnitude of this effect is dependent on the exact pulley dimensions for the finger, routing, and friction in the joints. In an effort to quantify this behavior for the different three-tendon designs, tests were undertaken to establish the proximal deflection when the medial phalanx is rotated through its extremes. After the initial of Design C and Design D, a new model is designed in which the pulley surfaces in the medial phalanx are offset, theoretically increasing the moment acting on that phalanx at extremes of motion. The results of the testing are provided in table 5 and table 6, with the theoretical range indicated from CAD models. All experiments were repeated several times to provide sufficient data and compensate the hysteretic behavior of PAMs.

Joint	Proximal	Medial
Design A	200°	120°

Joint	Proximal	Medial
Design B	200°	180°

Table 5: Range of movements achieved at each joint by designs A and B.

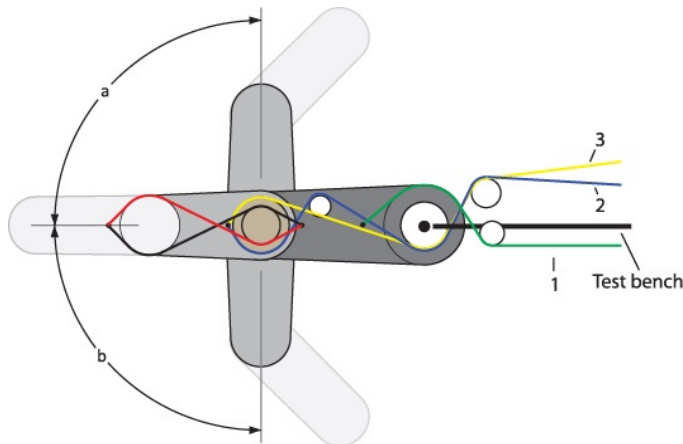


Figure 14: Proximal phalange in straight position

Qualitatively, it is seen that the bearings create a much smoother response and that the bearing design exhibits much more consistent behavior – the low friction is also observable when manually moving the finger, when compared to the non-bearing designs. To fix these last issues, a last model based on designs C and D has been designed.

Finger	Range on CAD	a	b	c	d	e	f
Design C	+/-87°	93°	93°	93°	90°	67.5°	90°
Design D	+/-100°	100°	92°	95°	100°	71°	70°
Unified Design	+/-87°	90°	85°	83°	90°	90°	89°

Table 6: Finger angle experiment results shown.

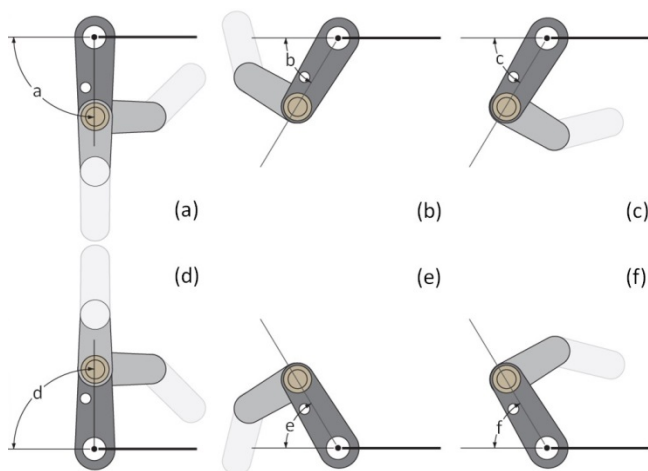


Figure 15: Finger position testing configuration.

### 3.1 Tendon Material

After reviewing the literature and researching viable materials the following list of fibres was compiled:

- Polyamide (Nylon) Type 66 30% carbon fibre
- Polyethylene Terephthalate (PET30) 310% long glass fibre
- Carbon Fibre (high strength grade) 5 micron f
- Carbon Fibre (High Mod Grade) 5 micron f
- ABS (10% stainless steel fibre)
- Dyneema (Spectra 1000/27micron dia)
- DuPont Kevlar 29 aramid fibre
- DuPont Kevlar 149 aramid fibre
- Aluminium Conductor Steel (Coated)

The selection process to find the tendon material to be used for the hand comprised of three phases:

Phase 1- Screening: A list of critical material

Design	Material Choice
Design A	Skeleton structure of the finger is made of solid steel Plates.
Design B	Aluminum Skeleton, Phalanges made up from two aluminum sheets, brass pulleys and rapid Prototyping parts printed from ABS plastic.
Design C	ABS plastic
Design D	Fused deposition modelling printed in ABS
Unified Design (Final)	Combination of best suited material used from all above designs

properties was drafted and critical performance values (CPV's) calculated. The selected materials properties were then compared to the 'critical performance values' and any material that failed to meet any of the critical criteria were discarded from the selection process.

Table 7: Material used in each design is shown.

Phase 2- Comparison: A weighted factor comparison matrix was composed using carefully selected material properties. Each property was then assigned a 'Weighting Factor' (WF) according to their importance. Each material property quantity was normalised by calculating each value as a decimal of the top scoring material in that category. The top scoring material in that category scores the value 1.0 and all others would score <1.0 depending on their value in relation to the top scorer. This normalised score (NS) is then multiplied by the WF in order to get the total score (Tot) for that material property. Each materials totals scores were then summed to give a Grand Total, the highest score indicating the material best suited to the application. Materials used in all designs are listed in table 7.

However, one significant omission of phase 2 is friction, highlighted as a major factor in the successful design of a robotic hand early in this project it could not be excluded from this analysis. It was also observed that whilst the materials database used for this analysis was extremely useful in narrowing down the search there is often a great difference between the idealised/generic properties it presents and those gained from genuine ‘off the shelf’ products. Hence an experimental study was also carried out to find the frictional properties of a small range of the most readily available materials from phase two. The top two materials: Kevlar and Dyneema (braided) along with a third: stainless steel carbo-flex (twisted), for variance,

were sourced. In all tests at higher loads the pulley shaft was visibly bowing and the tendon material in the case of the woven lines (Dyneema and Kevlar) showed some elongation as a result of braid alignment in the early loading stages. This was especially noticeable on the larger Dyneema. In the case of the larger 1.0mm Dyneema, this effect explains the much larger variation in coefficient of friction. Due to being much thicker, the tendon could not only withstand much higher loads, it also took longer and larger loads to fully align. Additionally, as it ‘aligned’ its CSA reduced which lowered its COF as it sunk into the groove. Problems found in each design are listed in table 8.

Design	Problems found in each design
Design A	The design proved useful as an initial test bed but didn’t achieve the full range of movement required due to following reasons: <ol style="list-style-type: none"> <li>1. Tendon wrapping was found to be a poor anti-lift method.</li> <li>2. Friction needed to be minimised and uniform where unavoidable.</li> <li>3. Securing tendons centrally using thread interference was found to be unsatisfactory.</li> </ol>
Design B	Even though the full range of movements is achieved, testing of the finger reveals some weak points of the structure. The sheet aluminium does not reach the required accuracy.
Design C	Overall performance of the finger was satisfactory; however further improvements of the design were required. These improvements were: <ol style="list-style-type: none"> <li>1. Increase the performance of the pulley controlling the movement of the Proximal Phalanx.</li> <li>2. Use of same size pulley with the variable radius which would increase the torque of the muscle in active mode and at the same time reduced the force of the muscle extension in the reverse motion.</li> <li>3. Implementation of the angular position sensors and the ball bearings into the finger joints to reduce friction.</li> </ol>
Design D	In order to maximise the performance of the finger, pulley diameters were chosen to utilise as much of the active range of the muscles as possible
Unified Design ( Final)	It met PDS constrains and no problem founded in the design.

Table 8: Problems faced at every stage are outlined.

Due to unknown frictions such as from the holding jig and the structure of the test rig these coefficients of friction can only be used for comparison with one another, which for the purpose of this exercise is perfectly acceptable. All of the tendon materials had a ‘settling in’ period for the first 20-25N which can be put down to movement/equilibrium of the structure. After that some relatively consistent results present themselves. The Dyneema 0.51 has the lowest coefficient of friction, followed by the Kevlar and then the dyneema 1.0. The fibre based tendons performed better than the stainless steel based carbo-flex, most likely as a result of their man-made synthetic fibres (Fig.16).

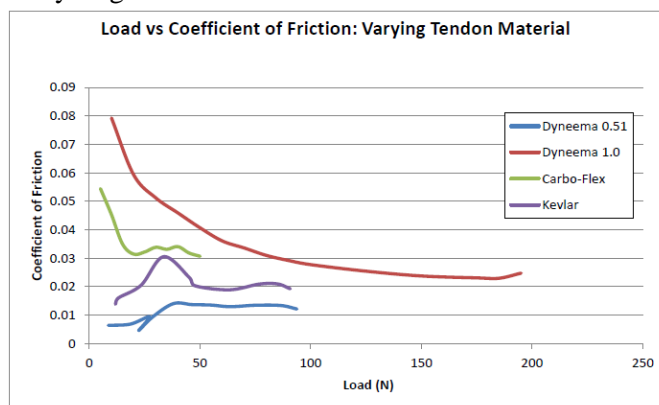


Figure 16- Load vs Coefficient of Friction Plots for four different tendon materials against a brass pulley.

Similar behaviour is observed in the pulley material tests with all materials exhibiting a ‘settling in’ period, although the period tends to be less distinct and the curve tends to take much longer to stabilise.

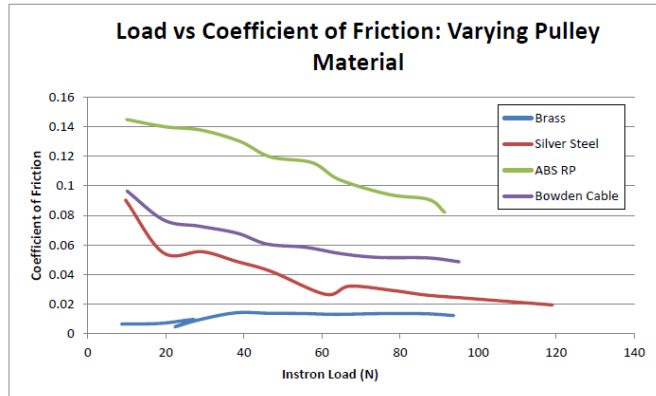


Figure 17- Load vs Coefficient of Friction plots for four different pulley materials against Dyneema 0.51 Tendon

The metal pulleys performed best with the self-lubricating brass having the lowest COF, in the case of the two metal pulleys the COF is primarily a function of their machinability. Brass is much easier to obtain a good finish with in comparison to the much harder silver steel which tends to rough up slightly more when turned. It is believed that the results would have been much closer had the pulleys not required turning (Fig.17).

Pulley Material	Std Dev	COF	Tendon Material	Std Dev	COF
Brass	0.003357	0.01336	Dyneema 0.51	0.003357	0.01336
Silver Steel	0.020804	0.028379	Dyneema 1.0	0.016074	0.025302
ABSRP	0.022379	0.101083	Kevlar	0.004429	0.021219
Bowden	0.014934	0.054084	Carbo-Flex	0.007634	0.03244

Table 9- Test Results: settled COFs and standard deviations.

Pulley Material (LHS), Tendon Material (RHS).

The Bowden cable had the third lowest COF and the RP plastic came last. As well as exhibiting higher COF’s the plastic materials also exhibit much larger ‘settling in’ periods, most likely a result of their inferior surface hardness leading to deformation of the top layer of the pulley as the load increases. It can be concluded that the tendon material with the lowest COF is Dyneema 0.51, showing a 58% reduction in COF over the worst performer- Carbo Flex. The pulley material that gives the lowest COF when combined with it is Brass, showing a massive 86.7% reduction in COF (compared to RP). This combination also heeded the most consistent COF under varying load with a comparatively small settling in period. The Brass pulley had a standard deviation of only 0.03, six times smaller than the second best performer silver steel, making it the best choice for control purposes too (Table 9).

The presence of the ‘system stabilisation’ has also led to the recommendation that in order to achieve the greatest accuracy with regards to tendon activation and control, the tendons need to be kept at a level of pre-tension to remove the effects of the settling in period. However, due to the system variables changing, length of tendon, route of tendon etc a value cannot be extrapolated from the results of this test alone.

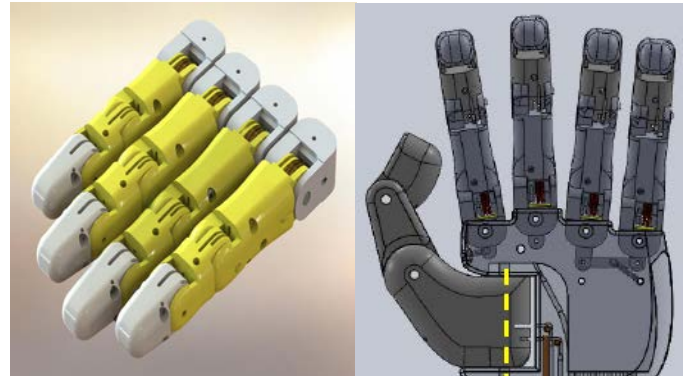


Figure 18: Final design of Fingers.

Testing also allowed observations of other material properties to be made regarding the tendon materials. Hence, it is concluded that braided lines have superior flexibility and excellent kink-resistance when compared to twisted lines. This property is particularly critical when considering the intricate routings that the tendons will be guided through. When bent around radii of 10mm and less the carbo flex tended to develop plastic kinks whereas the braided lines could be bent around as much as possible and showed no ‘memory’ whatsoever. Finally, taking the COF into account, the adjusted results of this comparison between the two remaining materials Kevlar and Dyneema (using Dyneema 0.51 COF as it is the closest in diameter to the 0.4mm Kevlar) show that Dyneema is the most applicable tendon material available (Table 10).

Kevlar	3.045
Dyneema	3.096

Table 10- Phase 3 Comparison Matrix Final Results.

Another important component of tendon choice was the tendon insertion method. Again, very little was found in the research/literature review and so an experimental study was carried out. However, since tendon insertion is highly dependent on the design itself the results were produced purely to inform the finger and thumb designs. It soon became apparent that the most likely finger/thumb material was to be FDM ABS plastic or some form of aluminum or steel plating. The latter being much stronger and stable, testing was restricted to methods involving Rapid Prototyped parts where the most uncertainty lie.



## CONCLUSION

Across the different prototypes presented in this paper, the concept of an ambidextrous robot finger has been designed tested and 3D printing of final design is completed (Fig.18). Four prototypes were presented in great detail. The design process started from choosing the right material to investigate tendons routing and improving overall design of the system by maximizing the range of muscles and designing with accurate geometrical features to rectify imperfection in previous designs. Flexibility and robustness of the system was optimized by analyzing the kinematic features of models. After initial testing to establish the kinematic ranges of the fingers, it was decided to proceed with an implementation of the three tendons routing schemes, implementing the offset pulleys in the medial phalanx base, but utilizing bearing-based joints.

Further research should aim to implement a similar spiral or offset pulley for the base of the proximal phalanx, with the intention of maximizing compression torque but minimizing the spring force of the muscle at the opposite extreme of motion. Another substantial requirement for the final design is to incorporate position sensing in the phalanx joints.

## Acknowledgments

This research was partially assisted by Shadow Robot Company Ltd (London, UK), which provided pneumatic and electronic devices, as well as technical assistance and hardware to control the first prototypes.

### References:

- [1] R. Balasubramanian and V. J. Santos, *The Human Hand as an Inspiration for Robot Hand Development*, vol. 95, Switzerland: Springer International Publishing, 2014.
- [2] J. L. Banks, "Design and Control of an Anthropomorphic Robotic Finger with Multi-point Tactile Sensation," Massachusetts Institute of Technology, Cambridge, 2001.
- [3] G. A. Bekey, R. Tomovic and I. Zeljkovic, "Control Architecture for the Belgrade/USC Hand in Dexterous Robot Hands," Springer-Verlag, 1999.
- [4] S. C. Jacobsen, E. K. Iversen, D. F. Knutti, R. T. Johnson and K. B. Biggers, "Design of the Utah/MIT Dexterous Hand," in *Proceedings of the 1986 IEEE International Conference on Robotics and Automation*, 1986.
- [5] C. Lovchik and M. Diftler, "The Robonaut Hand: a Dexterous Robot Hand for Space," in *Proceedings of the IEEE International Conference on Robotics and Automation*, Detroit, MI, 1999.
- [6] O. H. Penisi, M. Ceccarelli and G. Carbone, "Classification of Mechanisms for Industrial Fingers with Two fingers," *Iberoamerican Journal of Mechanical Engineering*, vol. 7 , pp. 59-75, 2003.
- [7] F. Y. Chen, *Gripping Mechanisms for Industrial Robots*, vol. 17, Mechanism Machine Theory, 1982, pp. 299-311.
- [8] J. Puig, N. Rodriguez and M.Ceccarell, "A Methodology for the Design of Robotic Hands," *International Journal of Advanced Robotic Systems*, vol. 5, pp. 177-184, 2008.
- [9] K. Salisbury and B. Roth, "Kinematics and force analysis of articulated mechanical hands," *Journal of Mechanims, Transmissions and Actuation in Design*, 1983.
- [10] T. William, "The Barrett Hand grasper-programmable flexible part handling and assemblyl," *Industrial Robot: An International Journal*, vol. Vol. 27, no. 3, pp. 181-188, 2000.
- [11] "Barret hand webpage," [Online]. Available: <http://www.barrett.com/>.
- [12] H. Kawasaki, H. Shimomura and Y. Shimizu, "Educational-industrial complex development of an anthropomorphic robot hand 'Gifu hand'," *Advanced Robotics*, 2001.
- [13] J. Butterfass, M. Grebenstein, H. Lieu and G. Hirzinger, "DLR-Hand II: Next Generation of a Dexterous Robot Hand," *Proceedings of the 2001 IEEE International Conference on Robotics and Automation*, pp. 109-114, 2001.
- [14] Y. Zhang, Z. Han, H. Zhan, X. Shang and T. & G. W. Wang, "Design and Control of the BUAA Four fingered Hand," *Proceeding of International Conference in Robotics and Automation*, pp. 2517-2522, 2001.
- [15] R. Soares and P. Grosch, "Dexterous Robotic Hand MA-I Software and Hardware Architecture," *Proceeding of Intelligent Manipulation and Grasping*, pp. 91-96, 2004..
- [16] F. Lotti, P. Tiezzi, G. Vassura, L. Biagiotti, G. Palli and C. Melchiorri, "Development of UB Hand 3: Early Results," *Proceedings of the 2005 IEEE International Conference on Robotics and Automation*, April 2005.
- [17] L. Zollo, S. Roccella, R. Tucci, B. Siciliano, E. Guglielmelli, M. C. Carrozza and P. Dario, "Biomechatronic Design and Control of an Anthropomorphic Artificial Hand for Prosthetics and Robotic Applications," *Proceeding of IEEE/RAS-EMBS International conference on Biomedical Robotics and Bio mechatronics*, 2006.
- [18] "ELU 2 Hand," [Online]. Available: <http://www.elumotion.com/Pdfs/Elu2-Hand-PR->

- 19-4-10.pdf.
- [19] "Shadow hand," [Online]. Available: [http://www.shadowrobot.com/wpcontent/uploads/shadow\\_dexterous\\_hand\\_technical\\_specification\\_E1\\_20130101.pdf](http://www.shadowrobot.com/wpcontent/uploads/shadow_dexterous_hand_technical_specification_E1_20130101.pdf).
- [20] H. B. et.al, "Evolution of Robotic Hands," University of Twente, 2010.
- [21] T. Laliberté, L. Birglen and C. Gosselin, "Underactuation in robotic grasping hands," Japanese Journal of Machine Intelligence and Robotic Control, vol. 4, no. Special Issue on Underactuated Robots, p. 77-87, September 2002.
- [22] F. Itoh and S. M, "Concept of underactuation". Japan Patent 75 151 397, 1975.
- [23] S. Hirose and Y. Umetani, "The Development of a soft Gripper for the Versatile Robot Hand," vol. 13, no. Mach. Theory, pp. 351-359, 1978.
- [24] S. Hirose and Y.Umetani, "The Kinematics and control of a soft Gripper for the Handling of Living or Fragile Objects," in Proc.5th Word Congress on the theory of Mechanics and Mechanisms, 1979.
- [25] T. Laliberte, L. Birglen and C. M. Gosselin, "Underactuation in robotic grasping hands," Machine Intelligence & Robotic Control, vol. 4, pp. 1-11, 2002.
- [26] K. a. S. I. Lee, "A Skeletal Framework Artificial Hand Actuated by Pneumatic Artificial Muscles," IEEE International Conference on Robotics and Automation ICRA99, Detroit, Michigan, 1999.
- [27] P. Scarfe and E. Lindsay, "Air Muscle Actuated Low Cost Humanoid Hand," International Journal of Advanced Robotic Systems, pp. 139-146, June 1, 2006.
- [28] A. P.-G. M. V. D. G. J.L. Sancho-Bru, "A 3D Biomechanical Model of the Hand for Power Grip," Journal of Biomechanical engineering, vol. 125, pp. 78-83, 2001.
- [29] M. V. W. Y. M. D.D. Wilkinson, " An Extensor Mechanism for an Anatomical Robotic Hand, vol.1, 2003, pp. 238-243," in Proc. IEEE International Conference on Robotics and Automation.
- [30] F. M. a. A. N. Y. Honda, "Control of pneumatic five-fingered robot hand using antagonistic muscle ratio and antagonistic muscle activity," in Proc. 3rd IEEE RAS & EMBS International Conference on Biomedical Robotics and Biomechatronics, 2010.
- [31] "Festo Exo-hand," 2012. [Online]. Available: [http://www.festo.com/cms/en\\_corp/12713.htm](http://www.festo.com/cms/en_corp/12713.htm).
- [32] "Shadow Dexterous Hand E1P1R, E1P1L," Shadow Robot Company Ltd, 2013. [Online]. Available: <http://www.shadowrobot.com/products/dexterous-hand/>.
- [33] I. M. Sousa, M. S. Couceiro, A. R. Barbosa, C. M. Figueiredo and N. M.F.Ferreira, "Exploiting the Development of Robotic Hands: A Survey and Comparison on Different Technologies," in IEEE 2nd International Conference on Serious Games and Applications for Health ( SeGAH), 2013.
- [34] A. Caffaz and G. Cannata, "The design and development of the dist-hand dextrous gripper," in IEEE International Conference on Robotics and automation , 1998.
- [35] N. Fukaya, S. Toyama, T. Asfour and R. Dillmann, "Design of the tuat/karlsruhe humanoid hand," in Proc. IEEE/RSJ Int. Conf. on Intelligent Robots and Systems, 2000.
- [36] S. Schulz, C. Pylatiuk and G. Bretthae, "A new ultralight anthropomorphic hand," in Proc. IEEE International Conference on Robotics and automation , 2001.
- [37] "bebionic 3," Liberating Technologies, Inc., [Online]. Available: <http://www.liberatingtechnologies.com>.
- [38] W. Fukui, F. Kobayashi and F. Kojima, "Development of Multi-Fingered Universal Robot Han with Torque Limiter Mechanism," The Future of Humanoid Robots- Research and Applications, 2012.
- [39] E. Akyürek, A. Dilly, F. Jourdan, Z. Liu, S. Chatteraj, I. B. Juandeaburre, M. Heinrich, L. Paramonov, P. Turner, Stelarc and T. Kalganova, " Remote-Controlled Ambidextrous Robot Hand Concept," Computer Technology ans Application (CTA), vol. 4, pp. 569-574, 2013.
- [40] E. Akyürek, T. Kalganova, M. Mukhtar, L. Steele, M. Simko, A. Nimmo, L. Kavanagh, A. Nimmo, A. Huynh and Stelarc, "Design and Development of Low Cost 3D Printed Ambidextrous Robotic Hand Driven by Pneumatic Muscles," International Journal of Engineering and Technical Research (IJETR), vol. 2, no. 10, pp. 179-188, Oct 2014.